Ordering Mechanisms in Epitaxial SiGe Nanoislands

G. Vantarakis,[1,2] I. N. Remediakis,[2] and P. C. Kelires[1]

[1]*Research Unit for Nanostructured Materials Systems, Department of Mechanical and Materials Science Engineering, Cyprus University of Technology, P.O. Box 50329, 3603 Limassol, Cyprus*

[2]*Department of Materials Science and Technology, University of Crete, P.O. Box 2208, 710 03 Heraklion, Crete, Greece*

(Received 11 November 2011; published 27 April 2012)

We investigate and elucidate the surprising observation of atomically ordered domains in dome-shaped SiGe nanoislands. We show, through atomistic Monte Carlo simulations, that this ordering is a surface-related phenomenon, and that is driven by surface equilibrium rather than by surface kinetics. The ordering depends on facet orientation. The main source of ordering is the {15 3 23} facet, while the {105} and {113} facets contribute less. Subsurface ordered configurations self-organize under this facet and are frozen-in and buried during island growth, giving rise to the ordered domains. Ordering mechanisms based on constrained surface kinetics, requiring step-mediated segregation at the island facets, are shown to be much less likely.

DOI: 10.1103/PhysRevLett.108.176102 PACS numbers: 68.35.Dv, 68.35.Gy, 68.47.Fg

During Ge on Si(100) heteroepitaxy, nanoislands of various shapes develop and self-organize [1]. Much work until today has been devoted to the elucidation of the composition profile in the islands due to intermixing and alloying [2–7]. The atomic distribution was thought to be random, much as like in bulk SiGe alloys [8,9], the prototypical semiconductor random alloy system.

Recently, however, a surprising observation was made. State-of-the-art x-ray diffraction studies clearly revealed, through analysis of basis-forbidden Bragg reflections, atomically ordered SiGe domains in dome-shaped islands [10]. The ordering is weak to moderate, it persists up to a growth temperature of 840 °C, having a maximum at 700 °C, and survives also under annealing conditions.

Ordering in SiGe systems has been earlier observed in $Si_{0.6}Ge_{0.4}$ superlattices [11] and thick relaxed $Si_{0.5}Ge_{0.5}$ films [12,13]. Although early kinetic considerations have linked ordering in such films to the formation of coherent islands during growth [13], the report of Malachias *et al.* [10] offers the first unambiguous sign of ordering at the nanoscale. The reduced size of three-dimensional islands, as compared to the practically infinite planar thin films, makes the appearance of ordering in nanometer-sized domains even more interesting, and opens up a number of questions regarding the underlying mechanisms, which remain elusive.

Here, we investigate in detail and explain this ordering effect. We show that the observed ordering in SiGe nanoislands is a surface-related phenomenon, and that is driven by surface equilibrium rather than surface kinetics. Moreover, we show that the ordering depends on facet orientation, which explains the observed spatial organization of the ordered domains in the islands. The ordering is of the mixed rhombohedral type.

The central idea is that ordering in nanoislands cannot be explained on the basis of *bulk equilibrium*, because this would lead to a random distribution of species. Similarly, *random kinetic processes* would also lead to a random alloy, if not accompanied by some surface site-specific selectivity. Thus, most likely ordering is due to surface-related processes, which are either driven by surface equilibrium [9,12] or by constrained surface kinetics [13].

In order to check the first possibility, we carry out Monte Carlo (MC) simulations of the equilibrium distributions of Si and Ge atoms in various facet configurations, and we calculate the degree of order at short and medium range. We check the second possibility by considering step-mediated segregation kinetic mechanisms at these island facets.

We begin with surface equilibrium. We study separately the {105}, {113} and {15 3 23} high-index surfaces, as these are the three most important facet orientations in SiGe dome islands grown on Si(100) [14]. A schematic of a dome island depicting the three facets is shown in Fig. 1(a). (i) The {105} surface has the rebonded S_B step (1×2) reconstruction [15]. It is vicinal to {100}, so dimers dominate the reconstruction. Two steps exist in the unit cell, one of which has the rebonded geometry with two adatoms. It is shown in Fig. 1(b). (ii) The {113} surface exhibits a (3×2) reconstruction, that involves an interstitial atom and an adatom [16]. The structure contains two nearly flat pentagons on the surface. It is shown in Fig. 1(c). (iii) The {15 3 23} surface is vicinal to {101}. It has an (1×1) reconstruction that involves three adatoms [17]. The relaxed structure is shown in Fig. 1(d).

We use simulational cells in a slab geometry with two surfaces (vacuum on top and bottom) and periodic boundary conditions. The slab cells are (6×6) repetitions of the unit cells. They contain 22, 19, and 21 monolayers (ML) and the total number of atoms is 10 100, 7632, and 9000 for the {15 3 23}, {105}, and {113} facets, respectively. The composition is kept at 50%–50% to be consistent

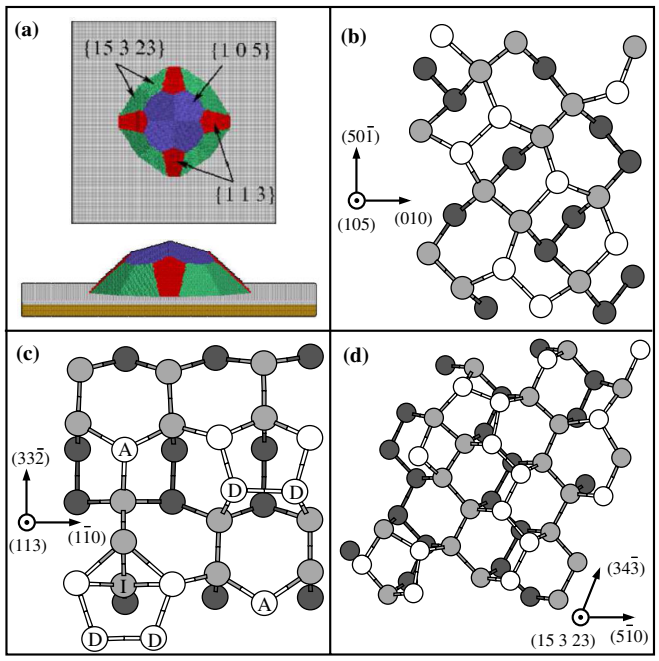

FIG. 1 (color online). (a) A multifaceted dome structure depicting the three facet orientations. (b) to (d) show the reconstructed {105}, {113}, and {15 3 23} facets, respectively.

with the experimentally measured [10] composition at the central region of the islands where ordered domains are seen. Epitaxial constrain of the lateral cell dimensions to Si(001) is imposed. Allowing them to vary changes the results insignificantly.

The systems are allowed to equilibrate, both geometrically and compositionally, using a continuous-space MC method that has been extensively tested in similar environments [3,9,18]. Three types of random moves are involved in the MC algorithm: atomic displacements and volume changes, which lead to geometrical relaxation, and mutual identity exchanges between atoms of different kinds, which mimic atomic diffusion and lead to compositional equilibration throughout the system. The energy is calculated using well-established interatomic potentials for Si/Ge [19].

We first present MC results for equilibrium at a low T, 100 K. This is artificial, since there is experimentally no diffusion to equilibrate at this T, but it unravels the maximum of the effect and provides a useful reference case before addressing the dependence on T up to high Ts.

Figure 2 shows pictorially local composition of the {15 3 23} facet system averaged over time (MC runs). We find that the surface is fully covered with Ge atoms due to the lower surface energy of Ge [9]. The same general effect is seen in the other two facets. Most notably, we observe that the distribution of Si and Ge atoms in the subsurface region strongly deviates from randomness. A clear tendency for clustering of atoms of the same kind in the subsurface layers is observed. A weaker clustering effect is seen in the other two facets (not shown).

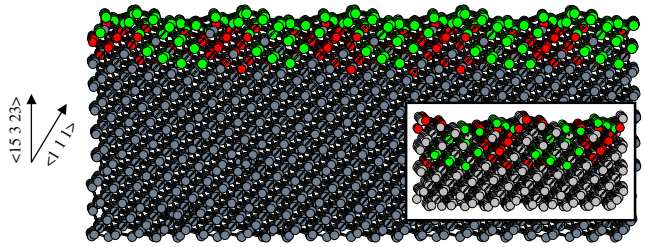

FIG. 2 (color online). Ball-and-stick model of local composition (based on Ge site occupancies) at the {15 3 23} facet. Red (dark grey) spheres are Si atoms ($c_{\mathrm{Ge}} \leq 0.25$), green (light grey) spheres are Ge atoms ($c_{\mathrm{Ge}} \geq 0.75$), while grey spheres are randomly occupied sites ($0.25 < c_{\mathrm{Ge}} < 0.75$). The inset shows the local stress distribution. Sites under compression (tension) are colored in red (green), while neutral sites (under less than ± 1 GPa) in grey.

The effect can be understood by noting that stress fields can trigger site-specific composition selectivity in alloyed systems, both at the surface and deeper in subsurface layers [9,12,20]. The inset in Fig. 2 shows atom-projected local stresses [9] in the {15 3 23} surface layers of pure Si. Several sites are under large stress exceeding 3–4 GPa, corresponding to a compression (tension) of more than 0.5 eV/atom, thus accessible to selective occupation, i.e., larger (smaller) atoms preferably occupy sites under tension (compression). A tendency for clustering of sites with similar stress state is observed, leading to favored occupation of these sites by the same kind of atoms.

Figure 3 shows stress variations as a function of depth in the three slab cells. In all three cases, there exists a thin subsurface layer (TSL) with large stresses, while deeper layers toward the middle of the slab are bulklike with minimal stress. The {15 3 23} system exhibits strong stress oscillations and thus selective site occupation at neighboring layers, while the {105} and {113} systems at more distant layers, which are separated by layers of low

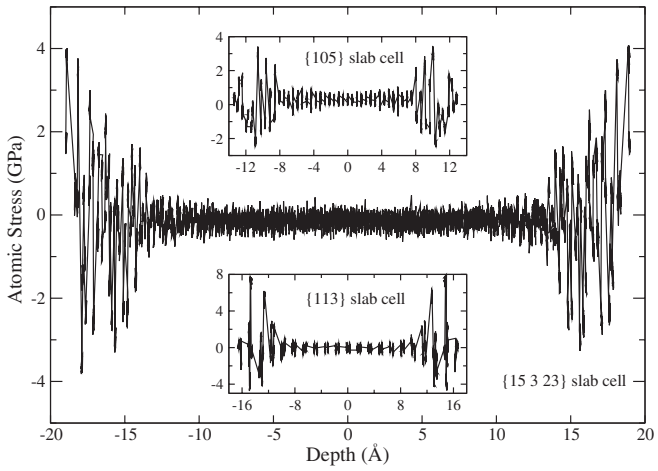

FIG. 3. Variations of atomic stresses versus depth in the three facet slab cells. The topmost surface layers are excluded.

stress and random occupation, thus the weaker clustering effect under these facets. The {15 3 23} TSL has a width of ~8 Å containing about four ML.

Analysis of local bonding in this TSL region shows that there is an abundance of local geometries in which three out of four bonds are either heteropolar or homopolar. These geometries are the basic building units of the RS1 and RS2 rhombohedral structures, respectively [8,12,21], characterized by ordered bilayers along a particular ⟨111⟩ direction. RS1 and RS2 have been extensively studied as candidate structures for long-range ordering in SiGe alloys [11,12,21]. Although both types of local ordered structures are found in the present case, the RS2 units are more numerous, indicating predominance of homopolar bonds, in accordance with the clustering picture in Fig. 2.

In order to quantify this first sign of ordering, we utilize the concept of the nearest-neighbor correlation parameter in a binary alloy, defined as $\Gamma_{AB} = c_A P_{AB} - c_A c_B$ [22], which relates the probability P_{AB} of a given bond being of type A-B, to the random case where each site are independently occupied with probability c_A or c_B (the compositions in the system.) Normalization of Γ_{AB} to maximum order results in the *Bethe* short-range order (SRO) parameter $\Gamma^{\mathrm{SRO}}_{\mathrm{Bethe}} = \Gamma_{AB}/(c_A P^M_{AB} - c_A c_B)$, where P^M_{AB} is the maximized probability. In the present case, $P_{\mathrm{Ge\text{-}Si}} = Z_{\mathrm{Ge\text{-}Si}}/4$, where $Z_{\mathrm{Ge\text{-}Si}}$ is the average number of heteropolar bonds in the structure, and $P^M_{AB} = 1$. For the zinc-blende, random, RS1 and RS2 structures, $\Gamma^{\mathrm{SRO}}_{\mathrm{Bethe}}$ equals to 1, 0, 0.5, and −0.5, respectively.

Analyzing in this way the SRO of the {15 3 23} facet, within the TSL with strong site preference, having an overall composition $c_{\mathrm{Ge}} = 0.4$, and excluding the fully covered with Ge atoms surface layer, we find a $\Gamma^{\mathrm{SRO}}_{\mathrm{Bethe}}$ value of −0.4, close to the value of the RS2 structure. This shows a high degree of SRO and confirms that the majority of local units are indeed of the RS2 type. The other two facets, {105} and {113}, exhibit a considerably lower degree of SRO, also characterized by a predominance of homopolar bonds, as is indicated by values of −0.2 and −0.14, respectively.

To examine whether order persists beyond the first nearest-neighbors and to trace its spatial extent in the TSLs, *albeit* laterally confined, we generalize the above formalism by defining a medium-range order (MRO) parameter $\Gamma^{\mathrm{MRO}}_{\mathrm{Bethe}}$. This is done by substituting for the bond probability P_{AB} the respective MRO probability P^{MRO}_{AB}, which correlates between sites in increasingly distant neighbor shells [23]. The results of this analysis for the three facets are summarized in Fig. 4(a). As a measure of the strength of MRO, we consider the deviations from the random level of zero. The strong oscillations of $\Gamma^{\mathrm{MRO}}_{\mathrm{Bethe}}$ of the {15 3 23} facet about the random level, though progressively declining, confirm that some type of order persists up to distant neighbor shells from the reference site. Weaker MRO is computed for the other two facets.

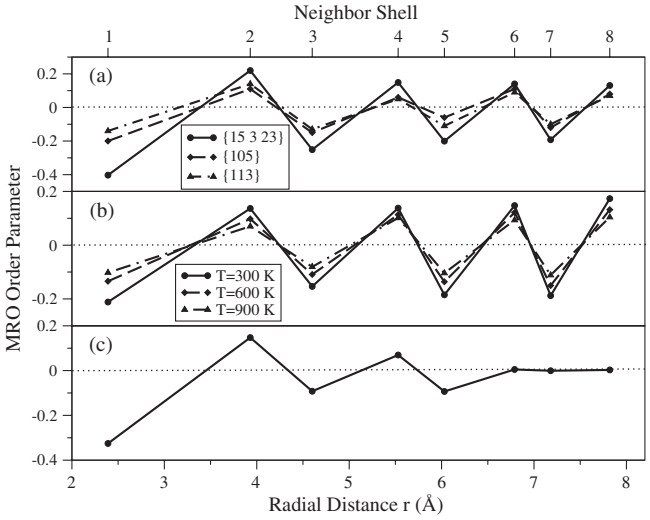

FIG. 4. (a) Variations of the medium-range order parameter $\Gamma^{\mathrm{MRO}}_{\mathrm{Bethe}}$ versus neighbor shells along the TSL of the three facets. Horizontal dotted line shows the random level. (b) MRO dependence on temperature for the {15 3 23} facet. (c) MRO in the periodic bulk model of the {15 3 23} structure.

Both the SRO and the MRO analyses indicate that the {15 3 23} facet is the main source of possible ordering in SiGe nanoislands.

Having demonstrated the effect at a low T, we now turn to higher Ts that are relevant to experimental growth conditions. For this, a series of MC simulations is carried out, extracting each time the MRO. Figure 4(b) shows MRO oscillations in the TSL of the {15 3 23} facet at higher Ts. MRO order persists even up to high Ts, where near surface diffusion is rapid.

To associate these results to the observed partial order in nanoislands [10], and to specify the type of ordering, we consider a periodic bulk model of the {15 3 23} structure, consisting of several repetitions of the TSL of 4 ML analyzed above, with sites "colored" as Si or Ge according to their average site occupancy. This model mimics an extended bulk domain under the facet, generated by assuming that surface configurations are frozen in and buried upon further material deposition during island growth [12,24].

Applying the *Bethe* analysis to this bulk {15 3 23} cell yields significant MRO, as shown in Fig. 4(c), extending up to the 5th neighbor shell. Beyond this distance, MRO falls off rapidly, characteristic of a cooperative assembly generating partial order. Because of the simplicity of the construction, this bulk MRO may only be considered as indicative of the strength and extent of order.

The RS1 and RS2 structures are not compatible to the computed MRO, either surface or bulk, RS2 being close only at short range [25]. This is in accord with the experiment [10], where no half-integer reflections (associated with RS1 and RS2) were observed. We conclude that the only possible structure to be associated with this ordering

is the mixed rhombohedral-type ordered structure RS3 [13,21], whose limiting cases are RS1 and RS2.

RS3 structures compatible with the computed MRO can be identified by fitting the Ge content in the alternating ordered ⟨111⟩ bilayers of the RS3 bulk model [21], so as to reproduce the calculated bulk $\Gamma^{\mathrm{MRO}}_{\mathrm{Bethe}}$. For this, we carry out Monte Carlo scans of the monolayer Ge content, allowing only identity exchanges within each layer. A fit to the partial order of the bulk cell, with a scan step of 0.2, yields a four-bilayer RS3 model with Ge contents (0.4, 0.6, 0.6, 0.8, 0.0, 0.2, 0.0, 0.2), composed of Si-rich, Ge-rich, and intermediate content layers. Similar configurational motifs emerge when considering other bulk models composed of TSLs of different thickness (2 or 6 ML).

Our theory explains many features of the observed weak ordering [10] and how this builds up in dome islands. First, it explains why ordered domains are seen in the central region of the islands, not at the bottom nor at the top. Bottom regions are Si rich due to macrostrain-driven intermixing, with composition $c_{\mathrm{Ge}} \simeq 0.2$, and thus RS3 cannot be formed as it requires near stoichiometry. In the center, $c_{\mathrm{Ge}} \simeq 0.5$, on average, and order is pronounced [10], but the lateral position of ordered domains is unknown. Also, simulational studies [24] of nonequilibrium faceted growth showed that there are in general strong lateral composition variations. These may affect ordering. Thus, we expect that partial RS3 order will rise up by the driving force of the $\{15\ \ 3\ \ 23\}$ facet as the island grows, in the central areas where the concentration is about 50%. The upper regions, on the other hand, remain Ge rich during growth and are bounded by {105} facets; see Fig. 1(a), which produce minimal order. This may also explain why ordering has not been reported for pyramidal islands; they are bounded by {105} facets.

Instead of a single area across the island, ordered domains separated by antiphase boundaries are seen. This can be explained by the argument that the {113} facets, which produce less order, intrude in between the $\{15\ \ 3\ \ 23\}$ facets, see Fig. 1(a), interrupting in this way the homogeneous formation of a single ordered domain.

In the observed ordering, a maximum appears as a function of T. This can be explained as follows: at low growth Ts diffusion in the subsurface region is slow and the system is not at equilibrium, with a low degree of order. With increasing Ts the facet system organizes into the equilibrium ordered structures. Higher Ts, however, tend to randomize the structure, reducing ordering and thus a maximum appears. Still a certain degree of order persists due to the high bulk diffusion barriers, when the ordered regions are buried, preventing its annihilation.

Finally, we consider an alternative ordering mechanism based on constrained surface kinetics [13]. This requires step-mediated segregation at the island facets. In this model, segregation during growth on double steps is vital, with kinks playing a key role in the process. It is well known that vicinal Si (100) surfaces usually include terraces separated by alternating S_A and S_B single steps when the miscut angle is low. Above 8°, however, double steps are favorable [26]. Yet, the Ge{105}/Si(001) facet [which forms an angle of about 11° with (001)] is well known to be stable due to a rebonded single-height step configuration [15,27]. Most importantly, the $\{15\ \ 3\ \ 23\}$ facet includes (110)-like features and resembles little similarity to (001) or its steps. Similar arguments apply to the {113} facet.

We conclude that the absence of double steps on the sides of $Si_{1-x}Ge_x$ dome islands makes the kinetic mechanism proposed by Jesson *et al.* [13] less likely. The effect of kinetics cannot be ruled out for small islands where edges between facets are close and might play the role of step kinks in the model of Jesson *et al.* [13]. Also, the {105} facet includes in every unit cell a feature resembling a S_B step that is only two atoms long. Yet, no ordering has been reported for pyramidal islands. Instead, our results give clear evidence that ordering is mainly due to thermodynamics of the growing facets rather than kinetics of the growth process.

This work was supported by the Cyprus University of Technology through generous start-up funding (P. C. K.).

[1] J. Stangl, V. Holý, and G. Bauer, Rev. Mod. Phys. **76**, 725 (2004).
[2] S. A. Chaparro, J. Drucker, Y. Zhang, D. Chandrasekhar, M. R. McCartney and D. J. Smith, Phys. Rev. Lett. **83**, 1199 (1999).
[3] P. Sonnet and P. C. Kelires, Phys. Rev. B **66**, 205307 (2002); Appl. Phys. Lett. **85**, 203 (2004); G. Hadjisavvas and P. C. Kelires, Phys. Rev. B **72**, 075334 (2005).
[4] A. Malachias, S. Kycia, G. Medeiros-Ribeiro, R. Magalhaes-Paniago, T. I. Kamins, and R. S. Williams, Phys. Rev. Lett. **91**, 176101 (2003).
[5] C. Lang, D. J. H. Cockayne, and D. Nguyen-Manh, Phys. Rev. B **72**, 155328 (2005).
[6] M. S. Leite, G. Medeiros-Ribeiro, T. I. Kamins, and R. S. Stanley Williams, Phys. Rev. Lett. **98**, 165901 (2007).
[7] U. Denker, M. Stoffel, and O. G. Schmidt, Phys. Rev. Lett. **90**, 196102 (2003); G. Katsaros, G. Costantini, M. Stoffel, R. Esteban, A M. Bittner, A. Rastelli, U. Denker, O. G. Schmidt, and K. Kern, Phys. Rev. B **72**, 195320 (2005).
[8] J. E. Bernard and A. Zunger, Phys. Rev. B **44**, 1663 (1991).
[9] P. C. Kelires and J. Tersoff, Phys. Rev. Lett. **63**, 1164 (1989).
[10] A. Malachias, T. U. Schulli, G. Medeiros-Ribeiro, L. G. Cancado, M. Stoffel, O. G. Schmidt, T. H. Metzger, and R. Magalhaes-Paniago, Phys. Rev. B **72**, 165315 (2005); M.-I. Richard *et al.*, Eur. Phys. J. Special Topics **167**, 3 (2009); A. Malachias M. Stoffel, M. Schmidbauer, T. Ü. Schulli, G. Medeiros-Ribeiro, O. G. Schmidt, R. Magalhães-Paniago, and T. H. Metzger, Phys. Rev. B **82**, 035307 (2010).

[11] A. Ourmazd and J. C. Bean, Phys. Rev. Lett. **55**, 765 (1985).
[12] F. K. LeGoues, V. P. Kesan, S. S. Iyer, J. Tersoff, and R. Tromp, Phys. Rev. Lett. **64**, 2038 (1990).
[13] D. E. Jesson, S. J. Pennycook, J. Z. Tischler, J. D. Budai, J. M. Baribeau, and D. C. Houghton, Phys. Rev. Lett. **70**, 2293 (1993).
[14] R. M. Tromp, F. M. Ross, and M. C. Reuter, Science **286**, 1931 (1999); Phys. Rev. Lett. **84**, 4641 (2000); A. Rastelli and H. von Kanel, Surf. Sci. **515**, L493 (2002).
[15] Y. Fujikawa, K. Akiyama, T. Nagao, T. Sakurai, M. G. Lagally, T. Hashimoto, Y. Morikawa, and K. Terakura, Phys. Rev. Lett. **88**, 176101 (2002); T. Hashimoto Y. Morikawaa, Y. Fujikawad, T. Sakuraid, M. G. Lagallyd, and K. Terakuraa, Surf. Sci. **513**, L445 (2002).
[16] J. Dąbrowski, H.-J. Müssig, and G. Wolff, Phys. Rev. Lett. **73**, 1660 (1994).
[17] Z. Gai, X. Li, R. G. Zhao, and W. S. Yang, Phys. Rev. B **57**, R15060 (1998).
[18] P. C. Kelires, Phys. Rev. Lett. **75**, 1114 (1995); Appl. Surf. Sci. **102**, 12 (1996).
[19] J. Tersoff, Phys. Rev. B **39**, 5566 (1989).
[20] F. Liu and M. G. Lagally, Phys. Rev. Lett. **76**, 3156 (1996).
[21] J. Z. Tischler, J. D. Budai, D. E. Jesson, G. Eres, P. Zschack, J. M. Baribeau, and D. C. Houghton, Phys. Rev. B **51**, 10947 (1995).
[22] J. M. Ziman, *Models of Disorder* (Cambridge University Press, Cambridge, England, 1979), p. 17; P. C. Kelires, Phys. Rev. B **55**, 8784 (1997).
[23] The average number of heteropolar bonds in the neighbor shells is extracted from radial distribution function analysis.
[24] X. B. Niu, G. B. Stringfellow, and F. Liu, Phys. Rev. Lett. **107**, 076101 (2011); Appl. Phys. Lett. **99**, 213102 (2011).
[25] The values of $\Gamma^{\mathrm{MRO}}_{\mathrm{Bethe}}$ for RS1 and RS2 vary with neighbor shell from ± 0.5, 0, to ± 1.
[26] E. Schröder-Bergen and W. Ranke, Surf. Sci. **259**, 323 (1991).
[27] V. Shenoy, C. Ciobanu, and L. Freund, Appl. Phys. Lett. **81**, 364 (2002); P. Raiteri, D. B. Migas, L. Miglio, A. Rastelli, and H. von Känel, Phys. Rev. Lett. **88**, 256103 (2002).